Computational and experimental verification of a wide-angle metamaterial absorber*

Chao Chen(陈超)[1,2,†] and Wang Jun(王君)[3]

[1] School of Computing Science, Sichuan University of Science & Engineering, Zigong 643000, China
[2] High Performance Computing Center, Sichuan University of Science and Engineering, Zigong 643000, China
[3] School of Science, Sichuan University of Science & Engineering, Zigong 643000, China

(Received 5 September 2016; revised manuscript received 24 November 2016; published online 20 February 2017)

A metamaterial absorber is computed numerically and measured experimentally in a 150-THz∼300-THz range. The measured absorber achieves high absorption rate for both transverse electric (TE) and transverse magnetic (TM) polarizations at large angles of incidence. An absorption sensor scheme is proposed based on the measured absorber and the variations of surrounding media. Different surrounding media are applied to the surface of the absorption sensor (including air, water, and glucose solution). Measured results show that high figure of merit (FOM) values are obtained for different surrounding media. The proposed sensor does not depend on the substrate, which means that it can be transplanted to different sensing platforms conveniently.

Keywords: sensors, metamaterials, simulation calculations

PACS: 41.20.Jb, 73.20.Mf, 42.25.Bs **DOI:** 10.1088/1674-1056/26/4/044101

1. Introduction

Artificially prepared electromagnetic metamaterial equipment has been widely computed and experimentally investigated since it has been confirmed theoretically and experimentally.[1–3] In practice, the exotic properties of electromagnetic metamaterial equipment usually attain from the unit cell structure designed scheme rather than constituent materials. Based on the exotic property, metamaterial equipment was used in a wide range, such as superlens, and absorber.[4–6] Especially, the metamaterial absorber has attracted a lot of research attention, since the metamaterial absorber was experimentally demonstrated by Landy *et al.*[7] To achieve absorption as high as possible, metamaterial absorber usually consists of many functional layers, including the electric resonator, dielectric interlayer, and metal reflector layer. The electric resonator and the metal reflector layer will couple separately in order to absorb as much incident electromagnetic wave as possible at resonance frequency.[8–14] Some research indicates that the absorption magnitude can be maximized when the impedance of the metamaterial absorber matches well to that of the free space air layer according to the effective mediums theory:[7,15]

$$z(f) = \sqrt{\mu_{\text{eff}}(f)/\varepsilon_{\text{eff}}(f)} \approx 1.$$

Metamaterial absorbers can beused in many fields, such as stealth technology, wavelength selective radiator, thermal imaging, and thermal bolometer.[7,11] In a wide frequency range, different structure designs of absorbers were used to achieve multi-band absorption.[7–10] Many existing metamaterial absorbers show dual-or triple-band absorption.[16–18] Up to now, the development of metamaterial absorbers has focused on the applications in the detection and sensing technology, because the absorption rate of the metamaterial absorber is easy to disturb when the refractive index of the surrounding medium is changed. For instance, the resonant nature of the localized surface plasmon, which always interferes with the incident electromagnetic wave and therefore affects the electromagnetic wave signal,[19] will be determined through the size, shape, and surrounding media of the metamaterial sensor.[20] It will limit the practical application range of the metamaterial sensor. In the actual detection and sensing applications, the variation of the surrounding media is an important key factor. In fact, many existing metamaterial sensors are optimized in order to reduce the influence of the wide range spectral variation in the surrounding dielectric media. These proposed structures mainly include nanostars, nanorice, and nanospheres.[21,22] However, in these existing proposed absorbers little attention is paid to the role of the variation of surrounding media.

In this paper, a simple structure metamaterial absorber is designed and fabricated, which consists of a circular-holes structured electric resonator, an MgF_2 dielectric layer, and continuous metal films. The perfect absorbing property of metamaterial absorber is studied by the effective medium theory and the computed currents. The metamaterial absorber

*Project supported by the National Natural Science Foundation of China (Grant No. 11547196), the Key Projects of Sichuan Provincial Department of Education, China (Grant No. 15ZA0224), the Project of Sichuan Provincial Key Laboratory of Artificial Intelligence, China (Grant No. 2014RYJ01), and the Key Plan Projects of Science and Technology of Zigong, China (Grant No. 2016CXM05).

†Corresponding author. E-mail: yujun_lly@sina.com

© 2017 Chinese Physical Society and IOP Publishing Ltd

shows high absorption rates in a wide incident angle range (0°–60°) in both transverse electric (TE) and transverse magnetic (TM) cases. Moreover, an absorption sensor scheme is suggested based on combining variation of the surrounding medium and the concept of the perfect absorber. The measured results show that the suggested absorption sensor scheme has a high sensitivity to the variation of the refractive indices of different surrounding media.

2. Model and results

Figures 1(a) and 1(b) show the design of the proposed matematerial absorber, and figure 1(d) displays the optical images. On the one hand, the proposed metamaterial absorber is fabricated through circular hole arrays in a square lattice. First, a silicon wafer is selected as a temporary substrate, and then a 400-nm thick SU-8 layer will be spun on the temporary substrate. A 45-nm thick gold layer is evaporated at a rate of 2.2 Å s-1 at the 58×10^{-10}-atm (1 atm = 1.01325×10^5 Pa) working pressure on the SU-8 layer as a bottom metal reflector by using the electron beam evaporation (Peva-600E). A 90-nm-thick MgF_2 intermediate medium layer is deposited on the first gold layer. Then, another 45-nm-thick top gold layer is evaporated on the MgF_2 intermediate medium layer (also using Peva-600E). The fabricated gold/ MgF_2/gold three-layers structured metamaterial (semi-finished products, not the final sample) is removed from the temporary Si substrate subsequently through adopting the buffered oxide etchant in order to etch the SU-8 layer away and liftoff the three-layers structured metamaterial. The gold/MgF_2/gold three-layers structured metamaterial is dried by using a C-MAG HP10 Hot plate (110 degrees Celsius, for 13 minutes). The purpose is to obtain an independent substrate absorber, which can be applied to a variety of sensor platforms conveniently. At the end, the proposed hole arrays are defined through adopting regular electron-beam lithography. The area of each sample is 2 mm×2 mm. The measured absorption result is obtained through the Bruker Optics Equinox spectrometer 55 Fourier transform infrared spectrometer. The optical images of samples are obtained through using a Leica DM2700M. On the other hand, the proposed metamaterial absorber is computed numerically by adopting Ansofts HFSS 11.0. The bottom gold layer is thick enough, which is larger than the skin depth of the incident light and therefore forbids the transmitted light through the samples. Therefore, the absorption rate can be obtained in simulations and experiments as follows: $A(f) = 1 - R(f)$. In simulations, the permittivity of the MgF_2 layer is set to be 1.9,[23] while the permittivity of bulk gold is set by the Drude model. In the Drude model, the damping constant is $\omega_c = 4.08\times10^{13}$ s^{-1}, and the plasma frequency is $\omega_{pl} = 1.37\times10^{16}$ s^{-1}.[24]

In this paper, the physical mechanism behind the absorption peak is explored by the simulation method. However, the difference between computed result and measured result naturally occurs, especially the damping constant of the Drude model plays an important role in the optical property of metamaterial. This is because the damping constant of the gold film is higher than that of the bulk gold due to the surface scattering and the grain boundary effect in thin metal film.[25] It is important to optimize the damping constant of bulk gold in simulation, in order to obtain the most realistic computed results. To obtain a most reasonable damping constant in the targeted scope (150 THz–300 THz) in this paper, simulated absorption peaks as a function of damping constants are shown in Fig. 2. It can be found that different amplitude absorption peaks are achieved with different damping constants. For the 1.0 time damping constant case (the black curve in Fig. 2), an absorption peak close to 95% at 212 THz is obtained. However, for the 1.06 times damping constant case (the red curve in Fig. 2), a maximum absorption rate close to 99.6% at 212 THz is obtained. This simulated result indicates that the damping constant equal to 1.06 times that in Ref. [24] can yield a high absorption peak resonance. Therefore, a simple structure designed perfect absorber is achieved. For 1.2 and 1.5 times cases (the green and blue curves in Fig. 2), the maximum absorbance rates are reduced to 87% and 65%, respectively. For different damping constants, the resonance frequencies are almost unchanged, while a maximum absorption rate can be obtained. It suggests that the optimization damping constant is important in simulation. Comparing these results of Figs. 1(c) and 2, it can be found that the computed result which is obtained under the 1.06 times damping constant is well consistent with the measured result in the 150-THz∼300-THz targeted spectrum. In the next results, the damping constants are all 1.06 times damping constants.

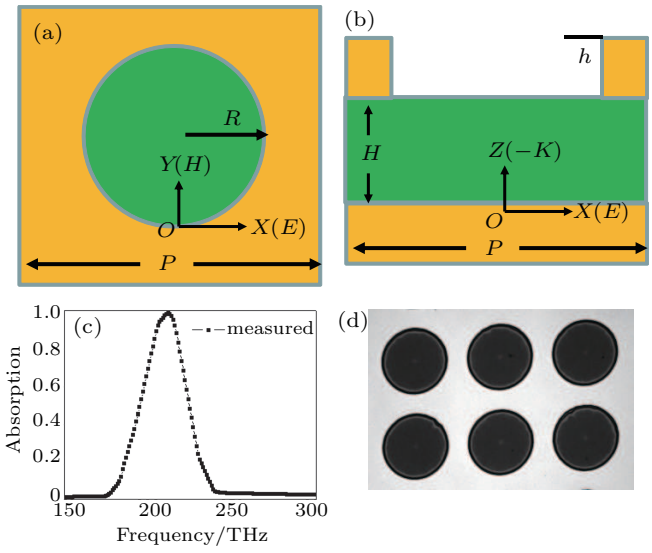


Fig. 1. (color online) (a) Top view of the unit cell on the XOY plane. (b) Side view of the unit cell on the XOZ plane. The orange part represents gold and the green part refers to MgF_2. (c) The measured absorption spectra. (d) Optical photos of samples.

Table 1. Dimension parameters of the proposed absorber.

Parameter	P	R	H	h
Value/nm	900	250	90	45

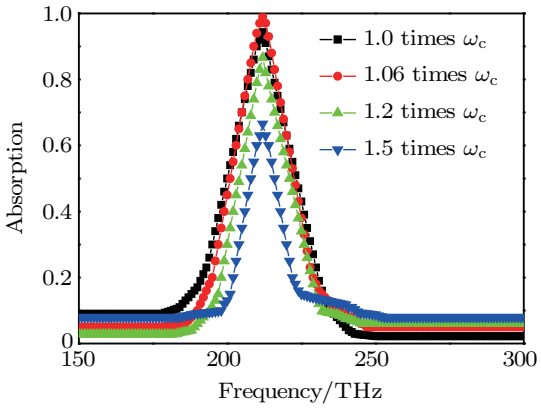


Fig. 2. (color online) Computed absorption peaks with different times damping constants of bulk gold.

The perfect simulated absorption peak in Fig. 2 (the red curve) indicates that the perfect impedance matching condition is achieved at the resonant frequency. Effective parameters (the effective permittivity and permeability) are extracted by using S parameters retrieval methods[26,27] as shown in Fig. 3. The real part of μ decreases from 18 to -15 in the absorption band, and crosses zero at $f = 212$ THz. At the same time, the real part of permittivity increases from -17 to 23 in the absorption band, and also crosses zero at the same resonant frequency. These computed results indicate the impedance match between the absorber and free air interface, which is similar to a previous result.[28]

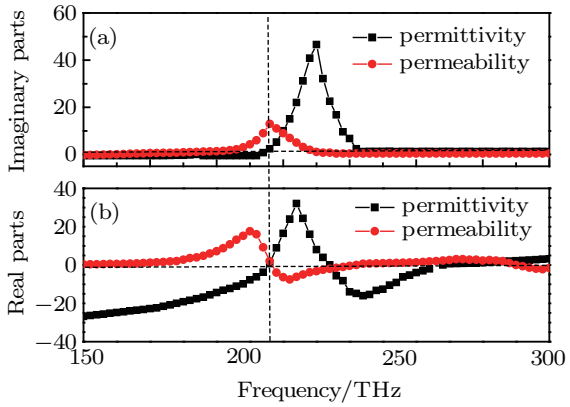


Fig. 3. (color online) (a) Imaginary parts of the effective parameters. (b) Real parts of effective parameters of the proposed metamaterial absorber.

In practice, the optical properties of the proposed absorber can be understood through the computed currents. Figure 4 shows the computed currents of the proposed absorber on the top and bottom gold layers at $f = 212$ THz. On the top gold layer, many parallel currents towards the right are excited. At the same time, many anti-parallel currents are also excited on the bottom gold layer. These resonant currents distribute on the bottom and top gold layers, which constitute a circulating current system. The circulating current system then excites a magnetic resonance field between the top and bottom gold layers at 212 THz, which interacts and couples with the incident light magnetic field.[29–31] The interacting and coupling phenomenon confines the incident light energy in the intermediate dielectric layer, which results in the absorption peak at 212 THz.

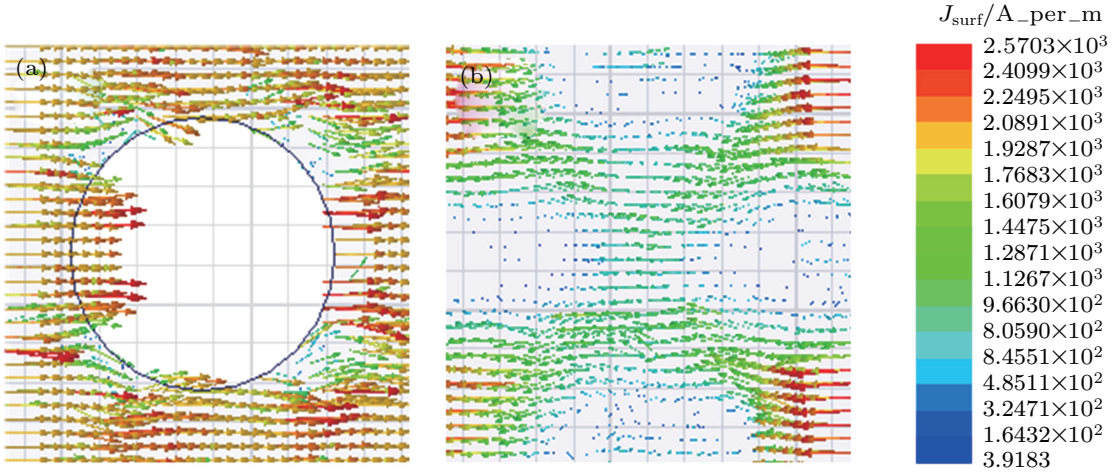


Fig. 4. (color online) Computed current distributions at 212 THz on (a) the top gold layer and (b) the bottom gold layer.

In this paper, the proposed metamaterials absorber is applied to various sensing platforms, such as photovoltaic cells, thermal emitters and detectors.[32,33] It is important to absorb as much of the incident light as possible when the proposed metamaterial absorber is used. Figure 5 shows the absorption spectra for both TM and TE configurations at various incident angles. For the case of the TM polarization, the maximum absorption rate is nearly unchanged (from 99.6% to 97.3%) with incident angle increasing. As discussed above, the direction of the incident resonance magnetic field is almost unchanged when the incident angle is increased, which will drive these circulating currents effectively at a large incidence angle as shown in Fig. 5(a). For the TE polarization case, resonant frequencies of absorption peaks are almost unchanged,

while the maximize maximum absorbance rate is reduced from 99.6% to 83%, as shown in Fig. 5(b). The abnormal decrease of the maximum absorption rate is due to the fact that the magnetic field cannot drive these circulating currents efficiently between two gold layers at a large incident angle.[34]

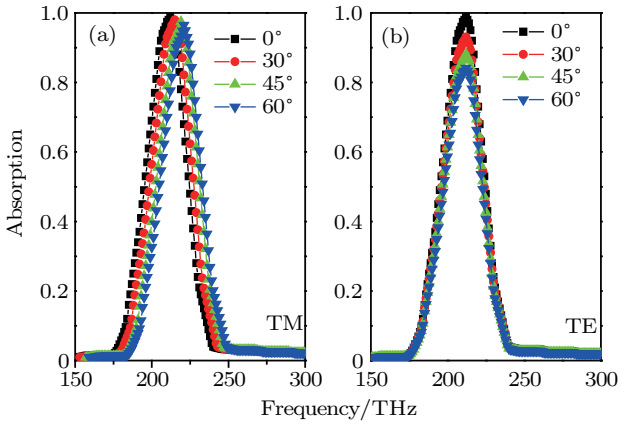


Fig. 5. (color online) Computed absorbance peaks for both TM and TE configurations.

In the following, the feasibility of the application to the sensor platform of the proposed metamaterial absorber will be discussed. The basic principle of the proposed absorption sensor is that the variation of the surrounding medium always plays an important role in the absorption rate. In practical applications, sensors always face different detection sensing environments. For instance, the surrounding medium on the sensor surface may change from air to water, or other media. When the sensing environment is changed, the refractive index of the surrounding medium on the sensor surface is thus changed, which causes the absorption rate to change. It is the opportunity for developing a sensor which is sensitive to detection and can sense the variation of the intensity in absorption when the refractive index of the surrounding medium is changed. Moreover, the proposed metamaterial absorber is independent of any substrate, which leads to the fact that the absorber can be applied to most sensor platforms.

To confirm the feasibility of the proposed absorption sensor above, three kinds of surrounding media (air, water, and glucose solution) are applied to the surface of the absorption sensor, and measured results are shown in Fig. 6(a). For the case of the air surrounding medium, the measured absorption peak reaches to 99.6%. When the air is replaced by the water surrounding medium, the measured absorption peak decreases to 97% (detection conditions are normal pressure and temperature). Finally, the water is replaced by the glucose solution surrounding medium (normal glucose solution for injection), and the measured absorption peak decreases to 93%. At the same time, the resonant frequency shows a shift toward low-frequency when the refractive index of the surrounding medium is increased. On the other hand, computed results are shown in Fig. 6(b). In these simulations, damping constants of gold layers are given as 1.06 times that of bulk gold. Moreover, the refractive index of surrounding media are given as $n_{\text{air}} = 1.0$, $n_{\text{water}} = 1.312$, $n_{\text{glucose}} = 1.322$, respectively. These computed results are well consistent with measured results.

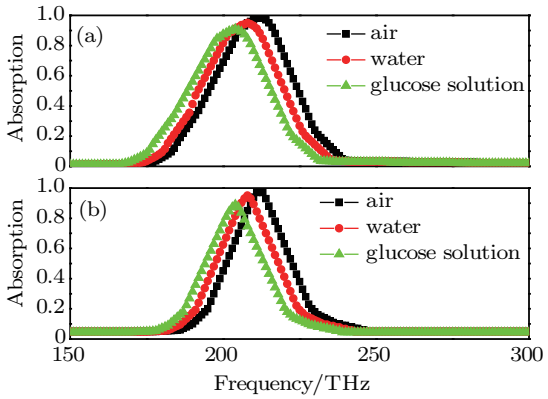


Fig. 6. (color online) (a) Measured and (b) computed absorption peaks with different surrounding media.

In order to evaluate the level of sensitivity on the variation of the refractive index of the surrounding medium, the figure of merit (FOM) is adopted to describe the performance of the absorption sensor in thefollowing. The FOM is given as

$$\text{FOM} = \max\left|\left[\frac{\mathrm{d}I(f)}{\mathrm{d}n(f)}\right]/I(f)\right|,$$

where $I(f)$ is corresponding to the intensity value at which the FOM reaches to the maximum value, $\mathrm{d}n(f)$ refers to the variation of the refractive index of the surrounding medium at which the FOM reaches to the maximum value, and $[\mathrm{d}I(f)/\mathrm{d}n(f)]$ represents the relative change of the absorption intensity, which is induced by a refractive index variation $\mathrm{d}n$ at a fixed frequency.[35] In practice, most exploited sensors measure the spectral shift of a resonance to detect the refractive index diversification of surrounding media.[36] However, this sensing principle is not very sensitive to the refractive index diversification of surrounding media because the variation of the resonance spectral shift is not considerable. On the other hand, the sensing principle of the proposed absorption sensor in this paper is to measure the change of the relative intensity $[\mathrm{d}I(f)/\mathrm{d}n(f)]$ with a refractive index variation $\mathrm{d}n$,[35] which can be characterized through the FOM value. Figure 7 shows the FOM values for different surrounding media. For the air surrounding medium case, a maximum FOM value around 164 is obtained at 228 THz, which is achieved at the resonant frequency when the $[\mathrm{d}I(f)/\mathrm{d}n(f)]$ (the computed FOM slope) is maximum. To expand the applications range of the proposed absorption sensor, the surrounding medium on the sensor surface will be changed into water and a glucose solution. For the water case, a maximum FOM value around 131 is obtained at 213 THz. For the glucose solution case, the maximum FOM value is 103 (the green curve in Fig. 7). Comparing these results of Figs. 6 and 7, it can be found that the maximum FOM

values of the water and the glucose solution are achieved not very exactly with resonant frequencies of absorption peaks. It is similar to a previous result.[35] The maximum FOM value of the proposed absorption sensor is obviously higher than that in Ref. [35], which implies that the level of sensitivity of the proposed absorption sensor is much higher.

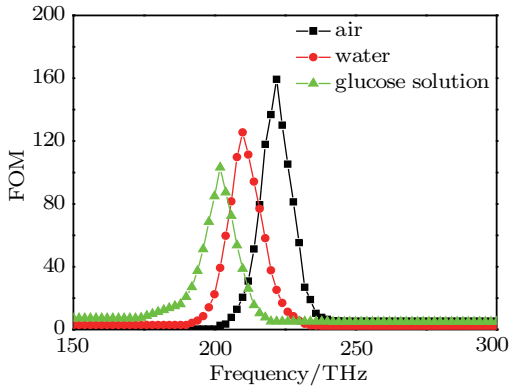


Fig. 7. (color online) Computed FOM value versus frequency for different surrounding media.

3. Conclusions

In this work, a metamaterial absorber is designed, computed, and measured in a 150-THz∼300-THz range. A perfect absorption peak is obtained at 212 THz. The measured absorber shows high absorption rates for the TM and TE polarizations at a large angle of incidence, for example 60°. Electromagnetic resonance properties of the measured absorber are analyzed through extracting effective parameters (the effective permittivity and permeability) and computing currents on the top and bottom gold layers at the resonance frequency. Moreover, the damping constant of bulk gold in simulation is optimized to obtain a most reasonable damping constant in the targeted scope (150 THz–300 THz) in this paper. Finally, an absorption sensor scheme is proposed through combining the measured absorber and the variation of surrounding media (including air, water, and glucose solution). Comparison among existing equipment shows that the proposed absorption sensor scheme is highly sensitive to variation of the surrounding media.

References

[1] Veselago V G 1968 *Sov. Phys. Usp.* **10** 509
[2] Pendry J B, Holden A J, Robbins D J and Stewart W J 1999 *IEEE Trans. Microwave Theory Tech.* **47** 2075
[3] Smith D R, Padilla W J, Vier D C, Nemat-Nasser S C and Schultz S 2000 *Phys. Rev. Lett.* **84** 4184
[4] Cheng B H, Lan Y C and Tsai D P 2013 *Opt. Express* **21** 14898
[5] Watts C M, Liu X and Padilla W J 2012 *Adv. Mater.* **24** OP98
[6] Wang Y T, Cheng B H, Ho Y Z, Lan Y C, Luan P G and Tsai D P *Opt. Express* **20** 22953
[7] Landy N I, Bingham C M, Tyler T, Jokerst N, Smith D R and Padilla W J 2009 *Phys. Rev. B* **79** 125104
[8] Tao H, Bingham C M, Pilon D, Fan K, Strikwerda A C, Shrekenhamer D, Padilla W J, Zhang X and Averitt D R 2010 *J. Phys. D: Appl. Phys.* **43** 225102
[9] Liu X, Starr T, Starr A F and Padilla W J 2010 *Phys. Rev. Lett.* **104** 207403
[10] Wen Q Y, Zhang H W, Xie Y S, Yang Q H and Liu Y L 2009 *Appl. Phys. Lett.* **95** 241111
[11] Landy N I, Sajuyigbe S, Mock J J, Smith D R and Padilla W J 2008 *Phys. Rev. Lett.* **100** 207402
[12] Cheng Y Z and Yang H L 2010 *J. Appl. Phys.* **108** 034906
[13] Hu C, Zhao Z, Chen X and Luo X 2009 *Opt. Express* **17** 11039
[14] Lee J and Lim S 2011 *Electron. Lett.* **47** 478
[15] Li M H, Yang H L, Hou X W, Tian Y and Hou D Y 2010 *Prog. Electron. Res.* **108** 37
[16] Cheng Y Z, Nie Y, Gong R Z and Yang H L 2011 *Eur. Phys. J. Appl. Phys.* **56** 31301
[17] Kreibig U and Vollmer M 1995 *Optical Properties of Metal Clusters* (Berlin: Springer)
[18] Stewart M E, Anderton C R, Thompson L B, Maria J, Gray S K, Rogers J A and Nuzzo R G 2008 *Chem. Rev.* **108** 494
[19] Lassiter J B, Aizpurua J, Hernandez L I, Brandl D W, Romero L, Lal S, Hafner J H, Nordlander P and Halas N J 2008 *Nano Lett.* **8** 1212
[20] Dmitriev A, Haegglund C, Chen S, Fredriksson H, Pakizeh T, Kaell M and Sutherland D S 2008 *Nano Lett.* **8** 3893
[21] Dodge M J. 1984 *Appl. Opt.* **23** 1980
[22] Ordal M A, Long L L, Bell R J, Bell S E, Bell R R, Alexander R W and Ward C A 1983 *Appl. Opt.* **22** 1099
[23] Zhang S, Fan W, Malloy K J, Brueck S R J, Panoiu N C and Osgood R M 2006 *J. Opt. Soc. Am. B* **23** 434
[24] Mary A, Rodrigo S G, Garcia-Vidal F J and Martin-Moreno L 2008 *Phys. Rev. Lett.* **27** 101103902
[25] Smith D R, Vier D C, Koschny T and Soukoulis C M 2005 *Phys. Rev. E* **71** 036617
[26] Liu X L, Starr T, Starr A F and Padilla W J 2010 *Phys. Rev. Lett.* **104** 207403
[27] Cai W S, Chettiar U K, Yuan H K, Silva V C, Kildishev A V, Drachev V P and Shalaev V M 2007 *Opt. Express* **15** 3333
[28] Fedotov V A, Mladyonov P L, Prosvirnin S L and Zheludev N I. 2005 *Phys. Rev. E* **72** 056613
[29] Schwanecke A S, Fedotov V A, Khardikov V V, Prosvirnin S L, Chen Y and Zheludev N I 2007 *J. Opt. A: Pure Appl. Opt.* **9** L1
[30] Ferry V E, Munday J N and Atwater H A 2010 *Adv. Mater.* **22** 4794
[31] Liu X L, Tyler T, Starr T, Starr A F, Jokerst N M and Padilla W J 2011 *Phys. Rev. Lett.* **107** 045901
[32] Tao H, Bingham C M, Strikwerda A C, Pilon D, Shrekenhamer D, Landy N I, Fan K, Zhang X, Padilla W J and Averitt R D 2008 *Phys. Rev. B* **78** 241103
[33] Becker J, Truegler A, Jakab A, Hohenester U and Soennichsen C 2010 *Plasmonics* **5** 161
[34] La S, Link S and Halas N J 2007 *Nat. Photon.* **1** 641
[35] Becker J, Truegler A, Jakab A, Hohenester U and Soennichsen C 2010 *Plasmonics* **5** 161
[36] La S, Link S and Halas N J 2007 *Nat. Photon.* **1** 641